Ovarian and placental morphology and endocrine functions in the pregnant giraffe (*Giraffa camelopardalis*)

S Wilsher, F Stansfield[1], R E S Greenwood[2], P D Trethowan[3], R A Anderson[4], F B W Wooding[5] and W R Allen

The Paul Mellon Laboratory, 'Brunswick', 18 Woodditton Road, Newmarket, Suffolk CB8 9BJ, UK, [1]The Elephant Conservation and Research Unit, Savé Valley Conservancy, Chiredzi, Zimbabwe, [2]Syde House, Saxon Street, Newmarket, Suffolk CB8 9RU, UK, [3]Department of Zoology, University of Oxford, South Parks Road, Oxford OX1 3PS, UK, [4]Queen's Medical Research Institute, MRC Centre for Regenerative Health, University of Edinburgh, 47 Little France Crescent, Edinburgh EH16 4TJ, UK and [5]The Physiological Laboratory, University of Cambridge, Downing Site, Cambridge CB2 3EE, UK

Correspondence should be addressed to S Wilsher; Email: pml777@virginmedia.com

Abstract

Gross, histological and immunocytochemical examinations carried out on maternal and fetal reproductive tissues from two pregnant giraffes at an estimated 8 and 13.5 months of gestation (term = 15 months) revealed a typically ruminant macrocotyledonary placenta with binucleate trophoblast cells scattered sparsely in the placentome where they stained intensely with a prolactin antiserum. Binucleate cells were present in greater numbers in the intercotyledonary allantochorion where they did not stain for prolactin whereas the uninucleate trophoblast still did. A single large corpus luteum of pregnancy and several small luteinised follicles were present in the maternal ovaries while the fetal ovaries at 13.5 months gestation showed an assortment of enlarging antral follicles and partially and completely luteinised follicles, the granulosa and luteal cells of which stained positively for 3β-hydroxysteroid dehydrogenase (3β-HSD), 17,20 lyase, prolactin, progesterone receptor and androgen receptor, but negatively for aromatase. The uninucleate trophoblast of the placentome and intercotyledonary allantochorion, the epithelium of the maternal endometrial glands, the seminiferous epithelium in the fetal testis at 8 months of gestation and the *zonae fasciculata* and *reticularis* of the fetal adrenal at 13.5 months also stained positively for 3β-HSD and negatively for aromatase. Endocrinologically, it appears that the giraffe placenta is more similar to that of the sheep than the cow with a placental lactogen as the likely driver of the considerable degree of luteinisation seen in both the maternal and the fetal ovaries.

Reproduction (2013) **145** 541–554

Introduction

With the paucity of post-mortem tissues for detailed study and the difficulty of serial sampling from live animals, little scientific attention has been directed towards the endocrine capabilities of the placenta in the giraffe, or to the morphology and relative roles of the maternal and fetal gonads in secreting protein and steroid hormones involved in pregnancy maintenance.

The morphology of the giraffe placenta has been described by a number of authors (Ludwig 1962, Wilson 1969, Hall-Martin & Skinner 1978, Deka *et al*. 1980, Hradecký *et al*. 1987, Mossman 1987, Benirschke 2007) who categorised it as a diffuse, macrocotyledonary, epitheliochorial organ occupying the entire uterine lumen, as in the majority of artiodactyl species. However, the ruminant placenta is now deemed to be synepitheliochorial in structure as the close but simple apposition of fetal trophoblast to maternal epithelium is modified by migration and fusion of trophoblast binucleate cells with the maternal epithelium throughout pregnancy (Wooding 1992).

The giraffe embryo always implants in the uterine horn ipsilateral to the corpus luteum (CL) and its placenta attaches to parallel rows of caruncles numbering around 60–70 in each uterine horn, with the resulting placentomes growing appreciably larger in the gravid than in the non-gravid horn. Histologically, each placentome is composed of elongated, minimally branched, interdigitating, fetal villi and accommodating maternal crypts. Binucleate cells within the trophoblast layer are much less numerous than in the placentae of the sheep, cow, deer and other artiodactyls and they tend to be congregated towards the tips of the fetal villi (Ludwig 1962, Benirschke 2007). It has not been determined whether fusion occurs between the binucleate trophoblast cells and the maternal epithelium to form the feto–maternal syncytia described in cattle and sheep by Wooding & Burton (2008). Nor has the production of

either steroid or protein hormones by the placenta been investigated, except for a cursory mention of placental lactogen activity in a giraffe term placenta by Forsyth (1986).

An unusual feature of pregnancy in the giraffe is hypertrophy of, and follicular and luteal activity in, the ovaries of the female fetus in late gestation. This was first reported by Kellas *et al*. (1958) who noted the presence of maturing, haemorrhagic and partly luteinised follicles in addition to a number of fully luteinised CL-like structures in the ovaries of two near-term female giraffe fetuses. They observed that the fetal ovaries in the giraffe were similar in appearance to those of an adult. The presence of these luteal structures in the fetal ovary was subsequently confirmed by Kayanja & Blankenship (1973), Gombe & Kayanja (1974) and Skinner & Hall-Martin (1975) and, more recently, Benirschke (2007) also noted multiple, small CL-like structures in the ovaries of an aborted giraffe fetus and a 3-day-old neonate. Such unusual developments in the fetal ovaries has led to speculation that the multiple CL-like structures may play a role in pregnancy maintenance, although the persistence of follicular growth and luteinisation after birth in the pre-pubertal giraffe (Kellas *et al*. 1958, Kayanja & Blankenship 1973, Gombe & Kayanja 1974, Hall-Martin & Rowlands 1980, Lueders *et al*. 2009*a*) would seem to argue against such a possibility. Interestingly, the newborn Okapi (*Okapia johnstoni*), the only other living *giraffid* species, does not display the same ovarian activity as the giraffe neonate (Bernirschke 2007). The testes in the male giraffe fetus have also been reported to undergo hypertrophy in late fetal life (Hall-Martin *et al*. 1978), although Benirschke (2007) found no evidence of interstitial cell stimulation in the testes of either the fetus or the neonate.

Only a single, large (3–5 cm diameter) pregnancy CL is present in one of the maternal ovaries and it persists throughout gestation (Amoroso & Finn 1962, Kayanja & Blankenship 1973, Hall-Martin & Rowlands 1980, Lueders *et al*. 2009*a*, 2009*b*). Progestins have been isolated from the ovaries of fetal, juvenile, pregnant and non-pregnant giraffe (Gombe & Kayanja 1974), and it was originally postulated that a placental gonadotrophin might be responsible for the follicular activity and luteinisation seen in the fetus (Kellas *et al*. 1958) following a report of gonadotrophic hormones in the urine of a pregnant giraffe by Wilkinson & De Fremmery (1940). However, Hall-Martin & Rowlands (1980) were unable to find any gonadotrophic activity in giraffe placental tissue and the continuation of follicular and luteal development in pre-pubertal giraffe ovaries also argues against involvement of a placental gonadotrophin (Gombe & Kayanja 1974, Lueders *et al*. 2009*a*). Although the adrenal gland of the giraffe fetus has not been investigated endocrinologically, Benirschke (2007) mentioned that it is unusually large and has a remarkably wide *zona fasciculata*.

The endocrine profiles of pregnant and non-pregnant giraffe have been investigated by measuring progestagens and/or oestrogens in faeces (Del Castillo *et al*. 2005, Dumonceaux *et al*. 2006, Isobe *et al*. 2007, Lueders *et al*. 2009*b*), urine (Lostutoff *et al*. 1986) and serum (Lueders *et al*. 2009*b*). Progestagen levels remain elevated throughout pregnancy (Dumonceaux *et al*. 2006) and then decline ∼3 days before parturition (Lostutoff *et al*. 1986). Isobe *et al*. (2007) measured faecal oestrogen and progestagen concentrations throughout gestation in a single female giraffe during two successive pregnancies but the profiles differed so much between the gestations that it was difficult to draw any conclusions.

The chance to recover fresh tissues from the gravid uteri of two pregnant giraffe culled for management reasons in a hunting conservancy in Southern Zimbabwe gave the opportunity for the present histological and immunocytochemical study to re-examine the gross and microscopic morphology of the placenta and the maternal and fetal gonads and to assess their hormone synthetic capabilities. Particular attention was paid to determine whether the fetal gonads may indeed contribute progestagens and/or other steroid hormones towards maintenance of the pregnancy state and whether the placenta might secrete a lactogenic hormone to drive luteinisation in the maternal and fetal ovaries.

Results

Gross fetal morphology

One giraffe (G1) was carrying a male fetus (G1F) with a crown-rump (CR) length of 60 cm and estimated weight of 15 kg (scales were not available at the time) and the second (G2) was carrying a female fetus (G2F) with a CR of 91 cm that weighed 37.46 kg. Based on these fetal weights, the known gestation length of 15 months in the giraffe (Benirschke 2007) and the data of Hall-Martin & Rowlands (1980), the gestational ages of the G1 and G2 fetuses were estimated to be around 8 and 13.5 months respectively.

The male fetus (G1F) was hairless, except for a few hairs on the switch of the tail, although the reticulation pattern was clearly visible on its skin. On the head, the eyelids were closed over the bulging eyes and the ears appeared fully formed. The hooves were soft and pale. The female fetus (G2F) was covered in hair and her coat colour was clearly visible. Mane and tail hair was present, vibrissae were protruding on the muzzle and the eyelids were fringed with eyelashes. The eyes were closed but were not as bulbous as the earlier specimen. Teeth were present in the lower jaw and ridged skin covered the hard palate. The tongue showed the typical dark pigmentation at its tip seen in adult giraffe.

Placentation

In both G1 and G2, the allantochorion occupied the whole of the uterine lumen (Fig. 1a). The placentomes were located in rows over the majority of the placenta with each composed of a fetal cotyledon, measuring up to 8 cm in diameter, interdigitated with its corresponding endometrial caruncle (Fig. 1a and b); the placentome was convex with respect to the fetal side (Fig. 1b). The large variation in size of the cotyledons was particularly evident in G1 in which large cotyledons of 4–6 cm diameter sat alongside tiny ones of <1 cm (Fig. 1a). These smaller placentomes were located at the tips of the uterine horns and on the uterine body cranial to the internal *os* of the cervix (Fig. 1a); the greater curvature of the allantochorion in the gravid horn was devoid of cotyledons (Fig. 1a). The fetal and maternal components of each placentome could be separated by steady manual pressure (Fig. 1c) whereas the intervening intercotyledonary allantochorion, which exhibited a vaguely stippled appearance (Fig. 1a and c), came away from the endometrial surface with almost no pressure at all.

The umbilical cord of G1F was 20 cm long and its outer surface was covered in numerous rough plaques; four vessels were evident on dissection. G2F's cord was similar in appearance, although somewhat longer at 42 cm. In both specimens, the cord was attached dorsally to the allantochorion. Numerous side branches vascularising individual cotyledons emanated from the major vessels that stemmed from the cord as it joined the allantochorion.

Histologically, each placentome consisted of simple, but very elongated and often convoluted, villi of allantochorion interdigitated with equivalently elongated

Figure 1 (a) The opened gravid uterus from G1 (8 months gestation) showing the dark red–brown fetal cotyledons of variable diameter on the body and lesser curvature of the allantochorion, but absent from the greater curvature in the gravid horn (divisions on rule=1 cm). (b) The allantoic surface of the allantochorion and its vasculature covering the convex placentomes (p) in G1 (scale bar=2 cm). (c) Manual pressure being applied to separate a placentome in G1 into its fetal and maternal components; ac, allantochorion; fc, fetal cotyledon; mc, maternal caruncle; endo, endometrium; my, myometrium (scale bar=1 cm). (d) Low-power section on one side of a small placentome (p) with overlying allantochorion (ac) from G1 showing the adjacent area of endometrium (endo) with numerous endometrial glands (asterisk) many of which are distended by cellular and secretory material accumulated in their lumina (scale bar=600 μm). (e) Low-power section at the maternal end of a placentome in G1 showing the thin and elongated strands of endometrial stroma rising up to interdigitate closely with villi of trophoblast passing downwards from the allantochorion (p, placentome; endo, endometrium; scale bar=200 μm). (f) Section near the fetal side of the placentome stained with the PR antiserum in order to differentiate maternal caruncle (mc) and fetal cotyledon (fc) tissues. Occasional binucleate cells (arrowed) can be seen in the trophoblast layer (scale bar=100 μm).

accommodating crypts in the maternal caruncle (Fig. 1e and f). The stroma of the maternal villi was denser, in terms of individual cells per area, than the fetal tissue (Fig. 1f). At both the maternal base and the opposite fetal chorionic plate of the placentome, it was possible to distinguish the layer of elongated and flattened maternal epithelial cells from the closely opposed layer of more cuboidal or columnar trophoblast cells of the allantochorion. However, this division into maternal and opposing fetal epithelioid layers was much less distinct in the central region of the placentome where thin cords of maternal and slightly broader cords of fetal stroma contained numerous capillaries to affect haemotrophic exchange.

In the endometrium on each side of the pedicle supporting the caruncle, clusters of endometrial glands were apparent (Fig. 1d), the distended lumina of many of them being filled with a coagulum of whole epithelial cells, cell debris, red blood cells (rbc) and exocrine secretion (Fig. 2f). Above these distended glands, the allantochorion was appreciably more convoluted (Fig. 1d) than further away in the intercotyledonary regions where it lay flat on the endometrial surface. No ferric iron could be detected by Perls' staining in these distended endometrial glands or, indeed, the whole of the placentome, whereas the haematogenous areas of a 17-month gestation elephant placenta stained with Perls' at the same time showed a strongly positive reaction.
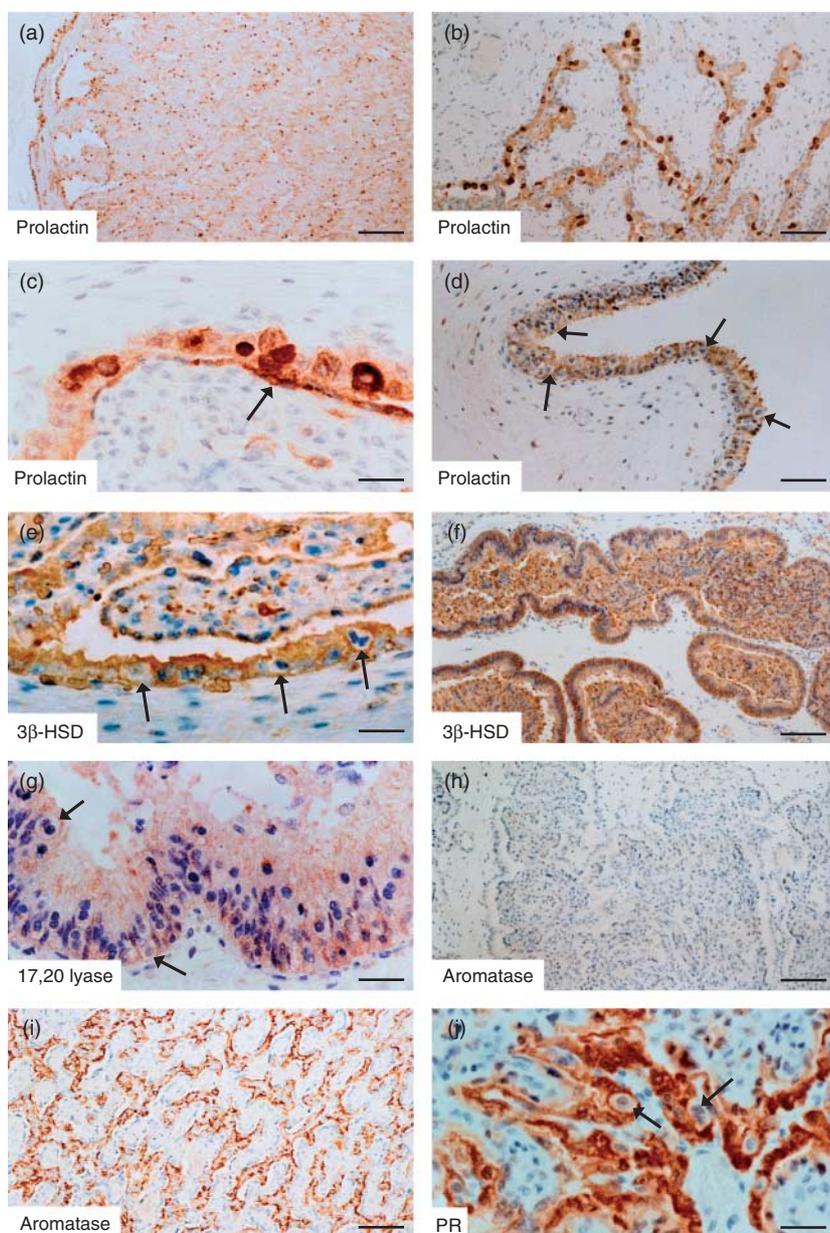
Figure 2 (a and b) Low- (a) and higher- (b) power sections of the fetal end of a placentome in G1 stained with the prolactin antiserum and showing the intensely stained binucleate cells scattered along the trophoblast, but with a tendency to be more densely accumulated towards the fetal end (scale bars a = 200 μm; b = 150 μm). (c) High-power section of the trophoblast–endometrium interface in a placentome in G2 stained with the prolactin antiserum. Note the patchy staining of the thin, elongated endometrial epithelial cells (arrowed) in close contact with the intensely stained binucleate trophoblast cells (scale bar = 40 μm). (d) Low-power section of the intercotyledonary allantochorion stained with the prolactin antiserum and showing the relatively dense accumulation of binucleate trophoblast cells (arrowed) which remain unstained in this region of the placenta (scale bar = 100 μm). (e) High-power section at the edge of a placentome of G1 showing positive staining of the uninucleate trophoblast by the 3β-HSD antiserum.
The binucleate cells (arrowed) remain unstained (scale bar = 40 μm). (f) Section of the distended endometrial glands at the lateral border of a placentome in G2 stained with 3β-HSD. The basal portions of the endometrial cells lining the glands stain strongly as does the secretory material adhered to the luminal surface of the cells and the accumulated coagulum, possibly as a result of 'stickiness' of the material (scale bar = 150 μm). (g) High-power section of the intercotyledonary region of the allantochorion in G1 showing positive staining of the cytoplasm of the uninucleate, but not binucleate trophoblast by the 17,20 lyase antiserum (scale bar = 40 μm). (h) Section at the fetal end of a placentome from G2 remaining unstained by the aromatase antiserum (scale bar = 150 μm). (i) Section of near-term sheep placenta showing strong, positive staining of the uninucleate, but not binucleate, trophoblast by the aromatase antiserum (scale bar = 150 μm). (j) High-power section at the fetal end of a placentome in G1 showing strong positive staining of the uninucleate trophoblast by the PR antiserum. The binucleate cells (arrowed) remain unstained (scale bar = 40 μm).

Division of the placentome into fetal and maternal components was better highlighted by staining with the prolactin, 3β-hydroxysteroid dehydrogenase (3β-HSD) and progesterone receptor (PR) antisera, all three of which stained one or more elements at the feto–maternal interface (Figs 1f and 2). Isolated, large binucleate cells that stained intensely with the prolactin antibody were present in the fetal trophoblast layer and, subjectively, these appeared to be slightly more concentrated towards the fetal end of the placentome (Fig. 2a and b). In contrast, the binucleate cells in the single layer of trophoblast covering the intercaruncle region of the allantochorion, although present in considerable numbers, were not stained by the prolactin antibody (Fig. 2d). The endometrial epithelium opposed to the trophoblast in the placentome also stained patchily with the prolactin antibody, especially those cells in close contact with the binucleate trophoblast cells (Fig. 2c). Although difficult to discern at the light microscope level, the impression was gained that these points may have represented areas where binucleate trophoblast cells had fused with the maternal epithelial cells in order to deliver their lactogenic hormone to the maternal circulation, as documented in cattle and other ruminant placentae by Wooding & Burton (2008).

Immunolocalisation of the 3β-HSD protein was demonstrated in the cytoplasm of the uninucleate trophoblast cells, but not in the binucleate cells (Fig. 2e). The capillaries within the placental tissue also stained positively, probably due to non-specific take-up of the chromagen by erythrocytes (Fig. 2e). The maternal component of the feto–maternal interface within the placentome did not stain with 3β-HSD. In contrast, the cytoplasm of the epithelium lining the dilated endometrial glands situated at the edge of the placentome did stain positively for 3β-HSD, with staining being very concentrated in the basal portion of the cells (Fig. 2f). In the distended glands, the apical portions of the lining epithelial cells were frequently covered by secretion, which stained intensely for 3β-HSD, as did the non-nuclear components of the material accumulated in the lumina of the glands (Fig. 2f). The 17,20 lyase enzyme was likewise immunolocalised to the cytoplasm of the uninucleate, but not the binucleate, trophoblast cells, both within placentomes and in the intercotyledonary regions (Fig. 2g). However, the aromatase antiserum did not stain any of the fetal or maternal components of the giraffe placenta (Fig. 2h), whereas it stained both sheep (Fig. 2g) and horse trophoblast strongly. The PR antiserum showed intense staining of both the nuclei
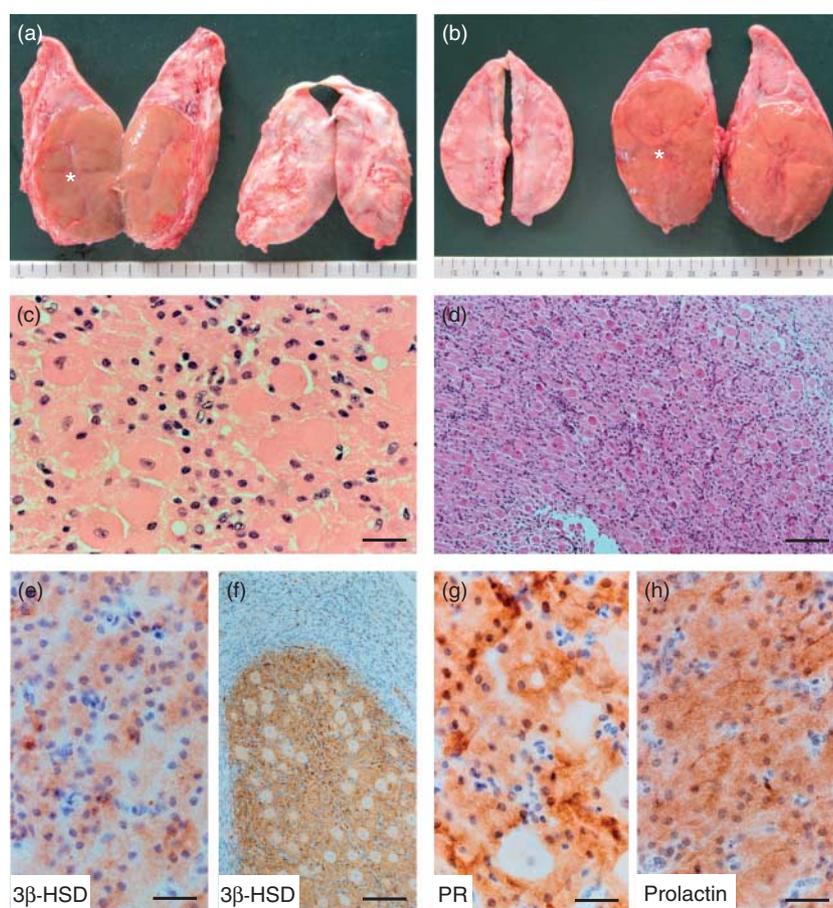
Figure 3 (a and b) The bisected maternal ovaries from, (a) G1 and, (b) G2 showing the single large corpus luteum (CL) of pregnancy (asterisk) occupying the majority of the volume of one ovary of each pair (divisions of rule = 5 mm). (c) High-power H&E-stained section of the pregnancy CL in G2 showing the mixture of large and small luteal cells, the latter with small, round dark-staining nuclei (scale bar = 40 μm). (d) H&E-stained section of the ovary of G1 showing an almost completely luteinised small follicle in the process of becoming an 'accessory CL' (scale bar = 100 μm). (e) Section of the pregnancy CL in G2 showing stronger staining of the small than the large luteal cells by the 3β-HSD antiserum (scale bar = 40 μm). (f) Section of a small 'accessory CL' in the ovary of G2 stained with the 3β-HSD antiserum. Note how the large luteal cells are much paler (scale bar = 150 μm). (g) High-power section of an 'accessory CL' in the ovary of G2 stained with the progesterone receptor (PR) antiserum. Isolated patches of small, but not large, luteal cells stain intensely (scale bar = 40 μm). (h) High-power section of the pregnancy CL in G1 showing positive staining of predominantly the large luteal cells by the prolactin antiserum (scale bar = 40 μm).

and the cytoplasm of the uninucleate trophoblast whereas, once again, the binucleate trophoblast cells remained unstained (Fig. 2j).

Maternal ovaries

The ovaries from G1 weighed 18.4 and 36.2 g and those from G2 weighed 17.3 and 67.6 g, the heavier ovary in each animal containing the single large, pale fawn-coloured CL of pregnancy, which comprised the majority of the ovary (Fig. 3a and b). The CL measured 3.5×5.0 cm in diameter in G1 at an estimated 8 months of gestation and 4.5×6.7 cm in G2 at an estimated 13.5 months. The luteal tissue was remarkably friable in texture, especially in G2. No large follicles were visible macroscopically, although several small dark spots in the medulla (Fig. 3a) were found histologically to represent small, partially or completely luteinised follicles (Fig. 3d and f).

Histologically, each pregnancy CL comprised a densely packed mixture of large and small luteal cells (Fig. 3c) and the cytoplasm of the large cells stained less intensely than the small luteal cells with the 3β-HSD antiserum (Fig. 3e). More strikingly, in the luteinised follicles that formed small 'accessory CL', the cytoplasm of the large luteal cells remained essentially unstained so that the more intensely stained small cells tended to

highlight the large cells scattered individually or in small clumps throughout the section (Fig. 3f). In the cortex, the primary, secondary and tertiary (antral) follicles showed positive staining for 3β-HSD, especially the cytoplasm of the granulosa cells. The 17,20 lyase antibody showed relatively weak staining of the luteal tissue with, once again, slightly darker staining of individual small luteal cells. As with the placenta, the aromatase antibody did not stain any of the ovarian tissue.

In the large primary CL of pregnancy in both G1 and G2, the PR antiserum stained the cytoplasm of a sub-population of the small luteal cells (Fig. 3g). Similarly, the PR antibody stained the small, but not the large, luteal cells in the small, partly and fully luteinised follicles scattered throughout the medulla. It also intensely stained the cytoplasm and nuclei of the granulosa cells lining the antral follicles. In addition, the prolactin antiserum also stained predominantly the large luteal cells in the maternal CL (Fig. 3h).

Fetal uterus and ovaries

The reproductive tract dissected from G2F showed the coiled uterine horns typical of ruminants (Mossman 1987) with long, well-defined oviducts traversing the mesovarium (Fig. 4a). The uterine lumen was filled with
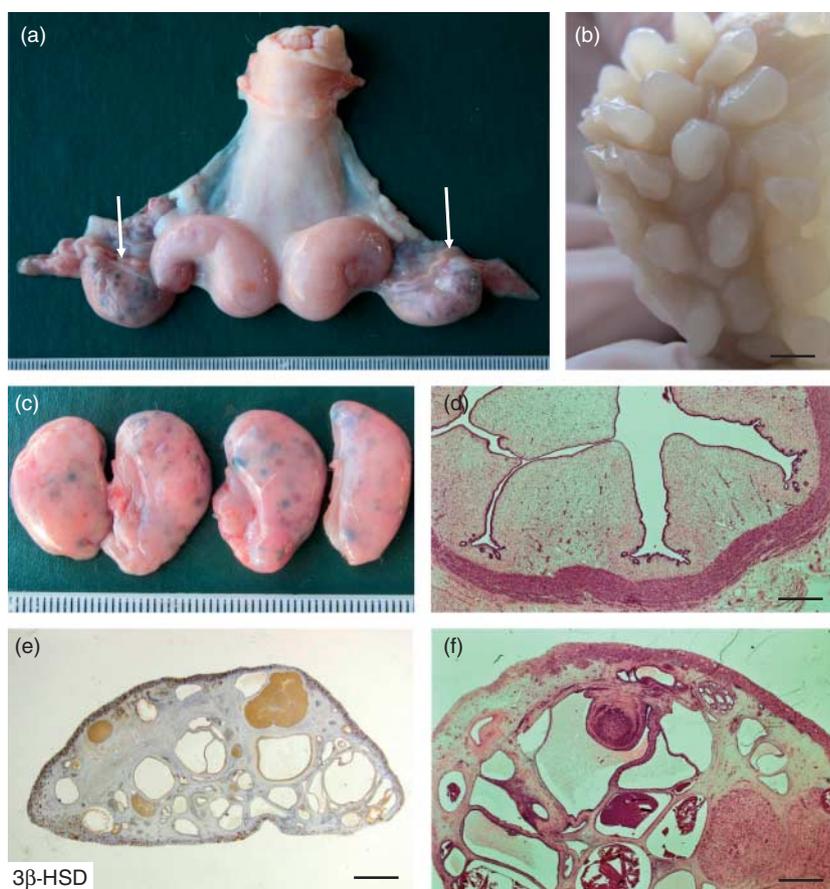

Figure 4 (a) The small undeveloped uterus and relatively enlarged ovaries from G2F with an estimated gestational age of 13.5 months. The oviducts are arrowed (scale in mm graduations). (b) The fetal uterus opened to show the lumen filled with rows of large, presumptive endometrial caruncles (scale bar=600 μm). (c) The bisected ovaries from G2F. Note the dark spots beneath the mesovarium revealing the blood-filled and luteinised antral follicles (scale in mm graduations). (d) Low-power section of a progenitor endometrial caruncle shown in (b). Note the shallow, rudimentary endometrial glands beginning to develop on either side at the base of each caruncle (scale bar=200 μm). (e and f) Photographs of histological sections of, (e) the left fetal ovary in G2 stained with the 3β-HSD antiserum and, (f) the right fetal ovary of G2F stained with H&E, both highlighting the jumbled mixture of enlarged antral follicles, many containing erythrocytes, and others partially or completely luteinised to form luteal structures of varying diameters (scale bars; e=350 μm, f=200 μm).

rows of relatively large presumptive endometrial caruncles (Fig. 4b). Each ovary weighed around 2 g and appeared enlarged in comparison to the development of the uterus (Fig. 4a). The external surface of both was smooth and showed a random distribution of multiple, dark haemorrhagic spots in the stroma beneath (Fig. 4c). When bisected before fixation, each ovary exhibited a variety of antral follicles and small luteal structures scattered throughout the medulla, which did not appear to have ovulated through the cortex and *tunica albuginea* (Fig. 4c).

Histological sections of the uterus showed the presumptive endometrium to be covered by a simple layer of epithelial cells, except at the base of the primitive caruncles where it was more convoluted and had begun to involute to form rudimentary endometrial glands (Fig. 4d). The cytoplasm of these luminal and glandular epithelia was stained positively by the 3β-HSD antiserum but not by the PR antiserum.

The fetal ovaries showed a clearly demarcated cortex packed with oocytes, the majority of which were organised into simple primordial or primary follicles (Figs 4e, f and 5a, c). The medulla beneath contained a mixture of well-developed antral follicles lined by granulosa cells, antral follicles filled with either rbc alone or a mixture of rbc and luteinising granulosa cells (Fig. 5b), and follicles that had undergone complete luteinisation to form small round or oval accessory CL-like structures that lacked any sign of an ovulation stigma (Figs 4e, f and 5a, b). In some luteinising follicles, the luteal
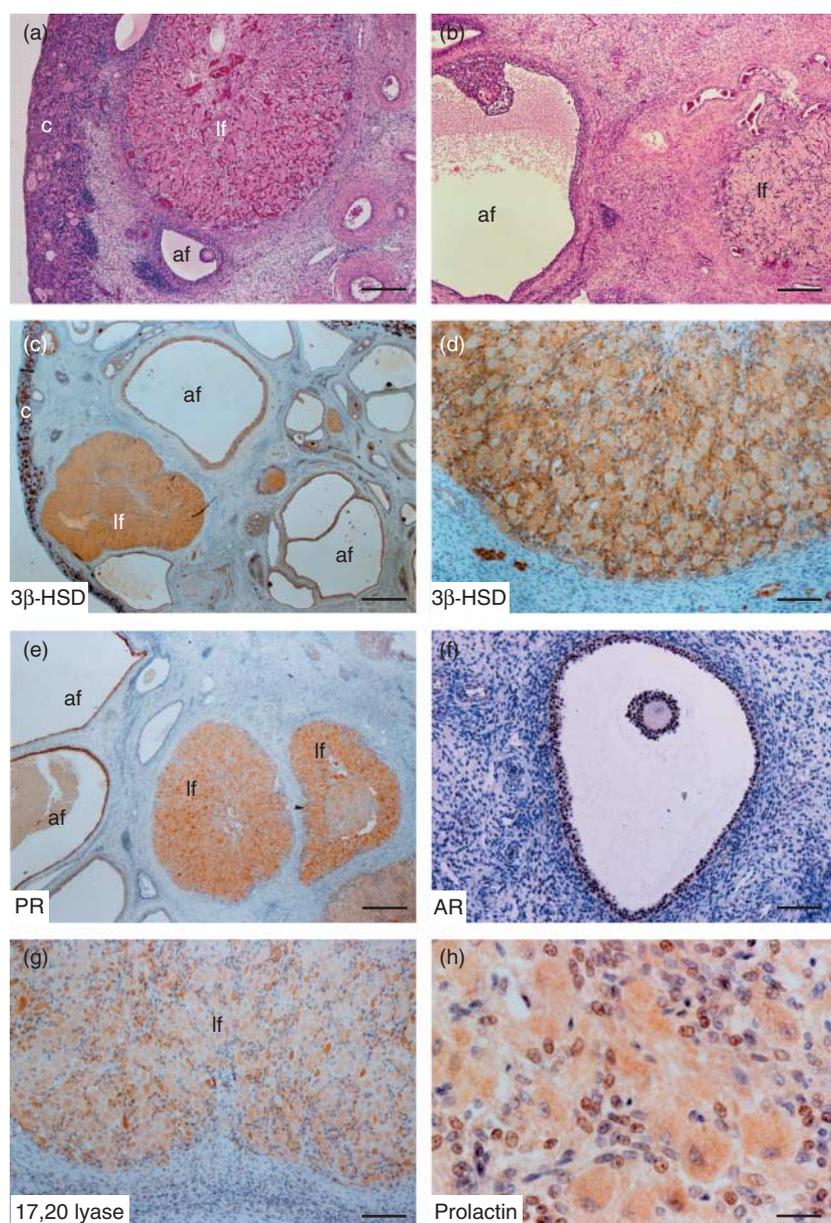
Figure 5 Sections of the ovaries from G2F at an estimated 13.5 months of gestation. (a and b) H&E-stained to show the cortex (c) packed with oocytes and small primary follicles, and the medulla containing antral follicles (af), a large af showing the first signs of luteinisation and fully luteinised follicles (lf: scale bar=175 μm). (c and d) Stained with the 3β-HSD antiserum. The granulosa cells of the primary follicles in the cortex (c) and those lining the antral follicles in the medulla (af) stain positively, as do the small, and to a lesser intensity the large, luteal cells of the lf (scale bars; c=200 μm, d=100 μm). (e) Lower-power section stained with the PR antiserum and showing strong staining of the granulosa layer of partially developed antral follicles (af) and large luteal cells in the lf (scale bar =200 μm). (f) Section of an antral follicle stained with androgen receptor (AR) antiserum and showing strong staining localised to the nuclei of the granulosa cells lining the follicle and surrounding the oocyte (scale bar=150 μm). (g) Section showing pale staining of the luteal cells, both large and small, in a lf by the 17,20 lyase antiserum (scale bar= 150 μm). (h) A lf showing positive staining of the cytoplasm of the large and the nuclei of the small luteal cells by the prolactin antiserum (scale bar= 40 μm).

tissue, composed of both large and small luteal cells, showed the characteristic folding of the luteinised granulosa and theca layers seen in the adult ovary after collapse of the ovulating follicle. Intense vascularisation was evident around the growing antral follicles and within the luteal tissue of the luteinised follicles (Fig. 5a and b).

The cytoplasm of the luteal cells in the fetal ovaries, like those in the maternal CL, stained positively with the 3β-HSD antiserum (Fig. 5c) and, as in the maternal ovary, the large luteal cells stained less intensely than the small ones interspersed between them (Fig. 5d); erythrocytes, both within and around the luteinised follicles, took up the chromagen non-specifically. The granulosa cells of the antral follicles also stained positively for 3β-HSD (Fig. 5c) and oocytes, whether present in partially developed antral follicles in the medulla or still in primordial and primary follicles in the cortex, also showed positive staining (Fig. 5c). The PR antibody labelled large luteal cells in the luteinised follicles and the granulosa cells lining the antral follicles (Fig. 5e). The nuclei of granulosa cells lining the antral follicles and surrounding the oocytes also stained

precisely with the androgen receptor (AR) antiserum (Fig. 5f); other structures within the fetal ovary did not show clear specific staining.

Both types of luteal cell comprising the CL-like luteinised follicles in the fetal ovaries stained weakly with the 17,20 lyase antibody, as did granulosa cells lining antral follicles in the medulla (Fig. 5g). The prolactin antiserum stained the cytoplasm of the large luteal cells and the nuclei of the small ones in the luteinised follicles in the fetal ovaries (Fig. 5h). It also bound to the granulosa cells in developing antral follicles and those lining the primordial, primary and secondary follicles in the cortex. As in the maternal ovaries, none of the tissues in the fetal ovaries, follicular, luteal or parenchymal, were stained by the aromatase antiserum.

Fetal testis

The small, undeveloped testes in G1F each weighed <1 g (Fig. 6a) and they had already descended fully into the rudimentary scrotum. Histologically, they
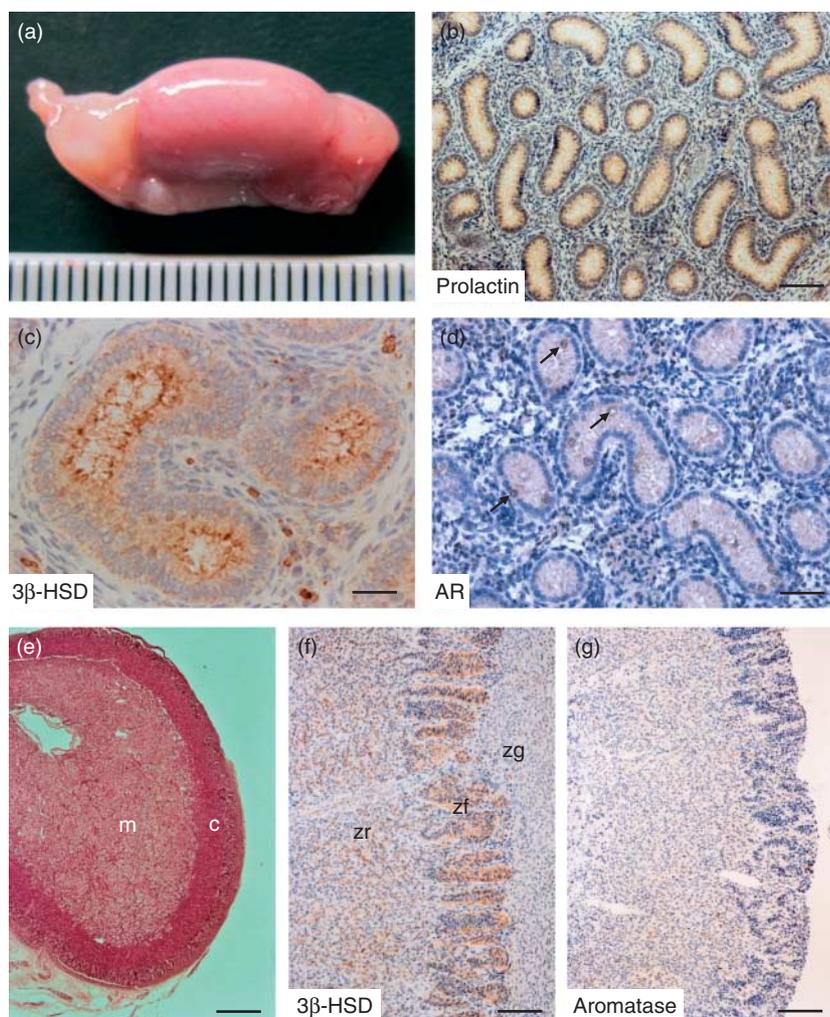
Figure 6 (a) A small testis and its epididymis recovered from the scrotum of G1F (scale in mm graduations). (b) Low-power section of the fetal testis showing pale staining of the seminiferous epithelium by the prolactin antiserum. The tubules are situated in a relatively dense and fibrous parenchyma (scale bar=150 μm). (c) High-power section of seminiferous tubules stained with the 3β-HSD antiserum and showing concentration of the chromagen in the apical portions of the epithelial cells. Small capillaries in the interstitium also take up the chromagen (scale bar=40 μm). (d) Section of the fetal testis showing negative staining of the seminiferous epithelium by the AR antiserum. Occasional round cells thought to be presumptive gonocytes are arrowed (scale bar=100 μm). (e) Very-low-power cross section of the adrenal gland from GF2 stained with H&E to highlight the cortex (c) and medulla (m: scale bar=5 mm). (f) Higher-power section showing positive staining by the 3β-HSD antiserum of cells in the *zona fasciculata* (zf) and less intense staining of those in the *zona reticularis* (zr). Cells in the *zona glomerulosa* (zg) are not stained (scale bar=150 μm). (g) Section of the adrenal gland from GF2 minus the outermost *zona glomerulosa* (artefactual). All the adrenal tissues remain completely unstained by the aromatase antibody (scale bar=150 μm).

exhibited a relatively dense accumulation of simple seminiferous tubules in the parenchyma, which were arranged in definite clumps separated by bands of interstitial cells and occasional strands of fibrous tissue carrying the blood vessels (Fig. 6b). The interstitial cells showed no signs of enlargement or clumping. Each tubule was lined by a single layer of tightly packed columnar epithelial cells within which were occasional large cells with round nuclei thought likely to be presumptive gonocytes (Fig. 6d). The epithelium was stained lightly by the prolactin antiserum (Fig. 6b) whereas their apical cytoplasm stained more intensely with the 3β-HSD antiserum (Fig. 6c). The 17,20 lyase antiserum also showed weak positive cytoplasmic staining of these seminiferous epithelial cells, whereas the PR, AR (Fig. 6d) and aromatase antibodies did not show positive staining.

Fetal adrenal gland

The adrenal gland from G2F measured ∼5 mm in diameter and 30 mm in length. Histologically, its cortex was typically composed of three distinct tissue layers (Fig. 6e). The outermost *zona glomerulosa* beneath the capsule consisted of small compact cells while the *zona fasciculata* underneath was composed of larger, epithelioid-type cells arranged in vertical columns or folds separated by capillaries. The inner *zona reticularis* made up the bulk of the adrenal cortex and it consisted of medium-sized, more loosely arranged flocculent cells interspersed with a rich capillary network. The adrenal medulla was also well vascularised and its cells were relatively large and pale staining (Fig. 6e). Within the cortex, the 3β-HSD and the 17,20 lyase antisera both stained some of cells in the *zonae fasciculata* and *reticularis*, both with more intensity in the former than in the latter; neither antibody stained the cells in the *zona glomerulosa* (Fig. 6f). The aromatase and PR antibodies did not stain any of the adrenal tissues (Fig. 6g).

Hormone measurements

Progestagen concentrations measured in both the maternal and the fetal sera and in the allantoic and amniotic fluids of G1 and G2 are shown in Table 1. Using the eCG assay, no gonadotrophic activity was detected in any of the maternal and fetal fluids.

Table 1 Progestagen concentrations measured in the maternal and fetal fluids of G1 and G2 pregnant giraffe.

Giraffe	Estimated gestational age (months)	Progestagen concentration (ng/ml)			
		Maternal serum	Fetal serum	Amniotic fluid	Allantoic fluid
G1	8	5.3	8.8	9.3	>30
G2	13.5	4.5	3.0	0.8	10.9

Discussion

In the two giraffes examined, the gross morphology of the placenta was very much as described by previous authors (Ludwig 1962, Wilson 1969, Hall-Martin & Skinner 1978, Deka *et al*. 1980, Hradecký *et al*. 1987, Mossman 1987, Benirschke 2007). As with the placentae of other ruminant species, binucleate trophoblast cells (Wooding & Burton 2008) were present and they were seen in both the cotyledonary and the intercotyledonary fetal membranes. Of particular interest was the finding of marginal folds of allantochorion at the base of each placentome situated above dilated endometrial glands that were frequently filled with a coagulum of cellular and secretory material. Although distended glands filled with debris of this type have not been described in other ruminants, Mossman (1987) observed that placentomes of all macrocotyledonary placentae have marginal folds of chorioallantois covered with phagocytic, columnar trophoblast cells, which may absorb the secretions of endometrial glands opening around the base of the caruncular pedicle. In addition, he stated that most of these absorptive areas are probably supplied with at least some extravasated maternal erythrocytes. Hence, it seems that the marginal regions of the placentome in the giraffe may represent a novel ruminant solution to providing maternal nutrients to the fetus by the breakdown and sloughing of hyperplastic endometrial gland epithelium into the lumen of the glands for subsequent absorption by the fetal trophoblast. However, the inability to detect ferric iron within the gland debris or in the trophoblast marginal folds suggests that if this is, indeed, a method of supplying histotroph, it does not include ferric iron and the possibility exists that the debris was accumulated in the gland lumina because their outlets were blocked. Interestingly, although not documented in ruminants, endometrial glands in the pregnant mole show sloughing and subsequent cytolysis of hypertrophied gland epithelial cells at the mouths of the glands with active phagocytosis by the specialised areolar trophoblast cells (Prasad *et al*. 1979, Malassiné & Leiser 1984, Enders & Carter 2006).

The maternal ovaries of both G1 and G2 exhibited a single large CL of pregnancy, thereby confirming the previous observations of Kayanja & Blankenship (1973), Hall-Martin & Rowlands (1980), Benirschke (2007) and Lueders *et al*. (2009*a*, 2009*b*). However, the ovaries also contained a number of small antral follicles with prominent thecal and granulosa cell layers plus atretic follicles with degenerating granulosa cells. In addition, there were a few small, completely luteinised follicles or 'accessory' CL, like those seen in the ovaries of G2F. Thus, luteinisation of relatively small and partly developed antral follicles was a prominent feature of both the maternal and the fetal ovaries in G1 and G2. In their original study of 27 pregnant giraffes, Kayanja & Blankenship (1973) reported only the single, large CL in

one of the two maternal ovaries with no mention of accessory CL, although they examined the ovaries only grossly. In contrast, Hall-Martin & Rowlands (1980) did mention accessory CL in pregnant giraffe ovaries but suggested that these structures occurred primarily in primiparous animals. In a more recent study using repeated transrectal ultrasonography examinations in captive giraffe, Lueders et al. (2009b) noted ongoing waves of follicular development during early pregnancy, with the largest follicle in each wave appearing to slowly regress rather than ovulate or luteinise. The small, multiple 'accessory luteal structures' observed in both the maternal and the fetal ovaries in this study may represent luteinisation of some of the follicles from follicular waves in early pregnancy that would have been too small to visualise ultrasonographically by Lueders et al. (2009a, 2009b). Alternatively, as appears to occur in the fetal ovary, small follicles may grow and become luteinised much later in pregnancy.

A previous report demonstrated that progestins were present in the extracts of homogenised giraffe ovarian tissue, both maternal and fetal (Gombe & Kayanja 1974). The immunohistochemical demonstration in this study of 3β-HSD, the enzyme required to convert pregnenolone to progestagens in the steroidogenic pathway, in the granulosa cells of developing follicles and luteal cells of both the maternal and the fetal ovaries highlighted the ability of these tissues to synthesise progestagens. The seminiferous tubule epithelium in the G1F testis at ∼8 months of gestation also showed evidence for an ability to synthesise progestagens, although whether enlargement of the fetal testes in later gestation, as suggested to occur by Hall-Martin et al. (1978), would result in the secretion of significant quantities of progestagens in the later stages of gestation remains unknown. Lostutoff et al. (1986) suggested that some of the progestagens required to maintain the pregnancy state in the giraffes, at least during the later stages of gestation, might originate from the multiple small accessory CL in the fetal ovaries. However, although there are clearly many of these accessory luteal structures in both the fetal and the maternal ovaries, their total volume would be much smaller than that of the single large maternal ovarian CL, which persists throughout gestation. Thus, it is hard to perceive that multiple 'accessory CL' in either or both maternal or fetal ovaries could supplant the pregnancy CL as the principle mainstay of the pregnancy state in the giraffe.

In the cow, cultures of isolated binucleate trophoblast cells have been shown to release progesterone (Reimers et al. 1985, Ullman & Reimers 1989) and, in the sheep and goat, isolated binucleate cells have the ability to convert pregnenolone to progesterone in the former and to 5β-pregnanediol in the latter (Wango et al. 1991). Furthermore, the latter authors could find no evidence that the uninucleate trophoblast cells played a significant role in progestagen synthesis is either species. In marked

contrast in the giraffe, the lack of 3β-HSD staining in the binucleate cells indicates their inability to convert pregnenolone to other steroids, whereas positive staining of the uninucleate trophoblast cells, particularly in the intercotyledonary regions, suggests they do possess progestagenic capacity. Hence, as in some ruminants such as the sheep (Mattner & Thorburn 1971), the placenta may well support, and even supersede, the maternal (and fetal) ovaries in secreting the progestagens to maintain the pregnancy state. The progestagenic function of the placenta would seem to be supported by the finding of significant concentrations of progestagens in the fetal fluids. On the other hand, measurement of peripheral serum progesterone concentrations throughout pregnancy in the giraffe have shown no obvious change in profile that might indicate when progestagens of placental origin may become a significant contributor to pregnancy maintenance (Dumonceaux et al. 2006, Isobe et al. 2007), if indeed they do.

Interestingly, both 3β-HSD and 17,20 lyase were immunolocalised to the glandular and luminal epithelia of the giraffe endometrium, suggesting that it too may be capable of synthesising progestagens and androgens in pregnancy. Although morphological and functional changes in the endometrial glands throughout the oestrous cycle and pregnancy are induced by steroids secreted by the ovary and/or placenta, localisation of 3β-HSD to the endometrium in women (Seki et al. 1987, Tang et al. 1993, Rhee et al. 2003), monkeys (Martel et al. 1994) and rats (Zaho et al. 1991) has led to the proposal that endometrial 3β-HSD is involved in the local metabolism of circulating steroids. If the endometrial glands in the pregnant giraffe are indeed synthesising steroids, it is reasonable to assume that these may act in an autocrine manner to stimulate the hypertrophy and hyperplasia noted in the epithelium of the endometrial glands clustered around the base of the placentomes. Certainly, the presence of the PR in this tissue suggests that progesterone plays a significant role in gland development and function in the pregnant giraffe. Furthermore, the presence of the PR on the trophoblast may indicate that progesterone is acting to regulate placental development and function in the giraffe, as has been proposed for the cow in mid-to-late gestation, although the pattern of expression differs markedly between the two species, with PR positivity limited to the stromal cells in the maternal caruncles in the cow (Schuler et al. 1999).

Hence, the positive staining for 3β-HSD of the accessory CL in both the maternal and the fetal ovaries, the seminiferous epithelium in the male fetus, the fetal adrenal and, particularly, the trophoblast of the placentomes and intercotyledonary areas and even the epithelium of the endometrial glands suggests that these many and diverse sources of progesterone synthetic capacity may contribute to the essential maintenance of the pregnancy state in the giraffe. Furthermore, the

presence of PR expression in some of the tissues indicates an autocrine role for these progestagens during pregnancy.

The giraffe placenta failed to stain positively with the aromatase antibody suggesting that, in contrast to the situation in the pregnant mare (Bhavnani *et al*. 1971) and ewe (Fevre 1967), but in a similar manner to the elephant (Allen *et al*. 2002), it does not secrete oestrogens. However, two reports (Isobe *et al*. 2007, Lueders *et al*. 2009*b*) have indicated that oestrogen is detectable during pregnancy in the giraffe. Early in gestation, the source of this oestrogen is most probably ovarian as fluctuating oestradiol levels at this time correspond the non-ovulatory follicular waves observed by Lueders *et al*. (2009*b*); it is not yet known whether these follicular waves persist past 90 days. However, the small size of the antral follicles seen in the maternal ovaries in this study would suggest that such follicular activity ceases in later pregnancy. Furthermore, no aromatase expression could be demonstrated in these small follicles, or indeed in those in the fetal ovaries, despite the fact that small quantities of oestrogen are usually produced by follicles during recruitment and selection in other species. Hence, the source of oestrogen detected in giraffe faeces in later pregnancy by Isobe *et al*. (2007) remains unclear.

In other ruminants, development of ovarian follicular activity and the tubular genitalia tend to occur in parallel during the post-natal, pre-pubertal period (Rawlings *et al*. 2003). The giraffe seems to be at odds with this general rule. For example, whereas the giraffe fetal uterus showed similarities to the bovine fetus in terms of development of the presumptive caruncles and rudimentary endometrial glands at the base of these structures (Atkinson *et al*. 1984), the giraffe fetal ovary, unlike that of the fetal calf, undergoes major antral follicle growth and luteinisation during at least the second half of gestation. Hence, whatever mechanism is driving these precocious activities in the ovaries is not simultaneously advancing endometrial gland development within the pre-natal uterus.

The gonadotrophic and luteotrophic stimuli for the hyperactivity in the giraffe fetal ovaries would probably come from the prolactin or lactogenic-like hormone being secreted by the uninucleate and, especially, the binucleate trophoblast cells within the placentome. Such production of one or more lactogenic hormones is a common feature of many artiodactyl, synepitheliochorial macrocotyledonary placentae (see Wooding & Burton (2008) for review), although the responses of both maternal and fetal ovaries to such stimulation seem to vary greatly between the species. For example, in the cow and goat, there is no evidence of fetal ovarian enlargement or follicular growth at any time during gestation and the maternal CL remains the principal, if not only, source of progesterone to maintain the pregnancy state until late in gestation, with the placenta remaining incapable of any serious progestagen synthesis

despite its high rate of placental lactogen secretion from an early stage (Antony *et al*. 1995). On the other hand, the sheep placenta synthesises both progestagens and oestrogens during pregnancy, to the extent that bilateral ovariectomy carried out as early as day 55 in the ewe is not followed by abortion (Fevre 1967). Nevertheless, the ovaries of the female sheep fetus show neither significant enlargement nor follicular/luteal development at any stage (McNatty *et al*. 1995). The question then arises as to why the placenta and fetal gonads in these various ruminant artiodactyls should respond so differently to what, on the face of it, is a basically similar mode of production of the same type of lactogenic hormone by the macrocotyledonary, synepitheliochorial placenta they all share (Wooding & Burton 2008). The range is thus from steroidogenic inertia of the placenta and fetal ovarian quiescence in the cow and goat, to full steroid capacity of the placenta combined with fetal gonadal quiescence in the sheep, to limited steroidogenic capacity of the placentae combined with a thoroughly impressive degree of follicular and luteal activity in the fetal ovaries in the giraffe. Like the giraffe, the equids and elephantids show fetal gonadal enlargement and steroidogenic activity during the second half of gestation (Bhavnani *et al*. 1971, Hay & Allen 1975, Allen *et al*. 2002). But despite this similarity, the endocrinology of pregnancy in all three of these genera differs greatly and, hence, provides no clear-cut pointers as to the mechanism driving fetal gonad enlargement, folliculogenesis and steroidogenesis.

In conclusion, this paper has provided further information on the steroidogenic capabilities of the placenta and maternal ovaries in the giraffe, along with those of the fetal gonads and adrenal cortex. Although it failed to unravel why the giraffe fetal ovaries should be so active during gestation, it has, nevertheless, demonstrated that the giraffe shows fascinating differences from other ruminants studied to date in its endocrinological management of pregnancy.

Materials and Methods

Animals

Two pregnant giraffes were killed by a single close-range neck shot from a heavy calibre rifle and the carcasses were transported to a small, purpose-built abattoir within 2 h of death. They were eviscerated while hanging vertically upside-down and the gravid uterus and ovaries were removed for further dissection and sample recovery.

Collection of tissues

The maternal ovaries were dissected and photographed, and half of the ovary containing the single CL of pregnancy was immersed in over 10 volumes of 10% (by volume) neutral buffered formaldehyde solution. Whole placentomes

Table 2 Primary antibodies used in the study.

Antibody specificity	Trade name	Source	Dilution	Manufacturer
3β-Hydroxysteroid dehydro-genase (3β-HSD)	3β-HSD (37-2): (sc-100466)	Mouse monoclonal raised against recombinant 3β-HSD of human origin	1:200	Santa Cruz Biotechnology, Inc.
17,20 lyase	P45017A1/cytochrome P450 17A1 (bs-6695R)	Rabbit polyclonal raised against a synthetic peptide derived from human P45017A1/cytochrome P450 17A1	1:100	Bioss Antibodies, Inc., Woburn, MA, USA
Cytochrome P450 aromatase	MCA2077S	Mouse monoclonal raised against a synthetic peptide corresponding to amino acids 376–390 of human aromatase	1:5000	AbD Serotec, Raleigh, NC, USA
Progesterone receptor (PR) (A and B forms)	NCL-PGR-AB	Mouse monoclonal raised against recombinant protein corresponding to the N-terminal region of the A and B forms of the human progesterone receptor	1:100	Novacastra Laboratories, Newcastle, UK
Prolactin	N1DDK-anti-hPRL-3	Rabbit polyclonal raised against human prolactin	1:9000	National Institute of Diabetes and Digestive and Kidney Diseases, Torrance, CA, USA
Androgen receptor (AR)	Ab74272	Rabbit polyclonal raised against N-terminal of human androgen receptor	1:200	Abcam Ltd, Cambridge, UK

consisting of the maternal caruncle and attached fetal cotyledon were dissected from the surface of the endometrium, taking care not to disturb the feto–maternal interdigitation. They were also immersed in buffered formaldehyde, as were pieces of endometrium and attached allantochorion recovered from the inter-placentome areas.

The abdomen of each fetus (one male and one female) was opened and the gonads and associated reproductive organs were dissected free. The testes or ovaries were recovered, bisected and immersed in fixative. In addition, the uterus and adrenal glands from one fetus were also fixed.

Histology and immunocytochemistry

The fixed tissues were trimmed and dehydrated through a graded series of alcohols before being embedded in paraffin wax for sectioning at 5 μm. The sections were either mounted on normal microscope slides and stained with haematoxylin and eosin (H&E) or Perls' stain (Churukian 2002) for conventional histology or layered onto positively charged slides for immunocytochemical staining. This was carried out using a Dako Autostainer whereby the sections were placed in a 56 °C oven overnight to dewax them. They were then immersed in a pre-heated (65 °C) bath of high-pH antigen unmasking solution (Dako PT link; Dako UK Limited, Ely, Cambs, UK) and heated to 97 °C for 20 min. After cooling, the slides were rinsed in neutral buffer and transferred to a Dako Plus Autostainer (Dako UK Limited) where a computer-controlled indirect staining method was performed. The optimally diluted primary and secondary antibodies were incubated for 30 min. The secondary antibody, blocking reagents, buffers, substrate, chromagen and nuclear stain were Envision FLEX reagents (Dako UK Limited) optimised for use in the Autostainer Plus. After staining, the slides were removed from the machine, dehydrated, cleared and mounted in DPX.

Details of the six primary antibodies used in this study are given in Table 2. Negative controls were run by replacing each primary antibody with an unrelated rabbit or mouse-generated antibody. In addition, equine, bovine, ovine, elephantid or human reproductive tissues known to stain negatively or positively with the antibody in question were used as further controls. The sections were examined under an Olympus Laborlux AH3 microscope (Olympus, Tokyo, Japan) and photographed using an integrated camera.

Hormone assays

Peripheral serum and allantoic and amniotic fluids were collected and assayed subsequently for progesterone concentrations and evidence of a placental gonadotrophin using the amplified enzyme-linked immunoassay (AELIA) described by Allen & Sanderson (1987) for progestagens and the AELIA assay for equine chorionic gonadotrophin described by Meadows et al. (1995).

References

Allen WR & Sanderson MW 1987 The value of a rapid progesterone assay (AELIA) in equine stud veterinary medicine and management. In *Proceedings of the 9th Bain-Fallon Memorial Lectures*, pp 75–82. Sydney: AEVA.

Allen WR, Mathias SS, Wooding FB, Skidmore JA & van Aarde RJ 2002 Placentation in the African elephant, *Loxodonta africana*. I. Endocrinological aspects. *Reproduction. Supplement* **60** 105–116.

Amoroso EC & Finn CA 1962 Ovarian activity during gestation, ovum transport and implantation. In *The Ovary*, p 451. Ed S Zuckerman. New York & London: Academic Press.

Antony RV, Liang R, Kayl EP & Pratt SL 1995 The growth hormone/prolactin gene family in ruminant placentae. *Journal of Reproduction and Fertility. Supplement* **49** 83–95.

Atkinson BA, King GJ & Amoroso EC 1984 Development of the caruncular and intercaruncular regions in the bovine endometrium. *Biology of Reproduction* **30** 763–774. (doi:10.1095/biolreprod30.3.763)

Benirschke K 2007 Giraffe (*Giraffa camelopardalis*). In *Comparative Placentation* http://placentation.ucsd.edu/giraffefs.htm. Accessed Nov 2012.

Bhavnani BR, Short RV & Solomon S 1971 Formation of estrogens by the pregnant mare. II. Metabolism of ^{14}C-acetate and ^{3}H-cholesterol injected into the fetal circulation. *Endocrinology* **891** 152–1157. (doi:10.1210/endo-89-5-1152)

Churukian CJ 2002 Pigments and minerals. In *Theory and Practice of Histological Techniques*, 4th edn, pp 243–268. Eds JD Bancroft & M Gamble. London: Churchill Livingstone.

Deka BC, Nath KC & Borgohain BN 1980 Clinical note on the morphology of the placenta in a giraffe (*Giraffa camelopardalis*). *Journal of Zoo Animal Medicine* **11** 117–118. (doi:10.2307/20094490)

Del Castillo SM, Bashaw MJ, Patton ML, Rieches RR & Bercovitch FB 2005 Fecal steroid analysis of female giraffe (*Giraffa camelopardalis*) reproductive condition and the impact of endocrine status on daily time budgets. *General and Comparative Endocrinology* **141** 271–281. (doi:10.1016/j.ygcen.2005.01.011)

Dumonceaux GA, Bauman JE & Camilo GR 2006 Evaluation of progesterone levels in feces of captive reticulated giraffe (*Giraffa camelopardalis reticulata*). *Journal of Zoo and Wildlife Medicine* **37** 255–261. (doi:10.1638/04-081.1)

Enders AC & Carter AM 2006 Comparative placentation: some interesting modifications for histotrophic nutrition – a review. *Placenta* **27** (Suppl A) S11–S16. (doi:10.1016/j.placenta.2005.10.013)

Fevre J 1967 Urinary oestrogens in the ovariectomized pregnant ewe. *Annales de Biologie animale Biochimie, Biophysique* **7** 29–32. (doi:10.1051/rnd:19670103)

Forsyth IA 1986 Variation among species in the endocrine control of mammary growth and function: the roles of prolactin, growth hormone and placental lactogen. *Journal of Dairy Science* **69** 886–903. (doi:10.3168/jds.S0022-0302(86)80479-9)

Gombe S & Kayanja FIB 1974 Ovarian progestins in Masai giraffe (*Giraffa camelopardalis*). *Journal of Reproduction and Fertility* **40** 45–50. (doi:10.1530/jrf.0.0400045)

Hall-Martin AJ & Rowlands IW 1980 Observations on ovarian structure and development of the Southern giraffe, *Giraffa camelopardalis giraffa*. *South African Tydskr Dierk* **15** 217–221.

Hall-Martin AJ & Skinner JD 1978 Observations on puberty and pregnancy in female giraffe (*Giraffa camelopardalis*). *South African Journal of Wildlife Research* **8** 91–94.

Hall-Martin AJ, Skinner JD & Hopkins BJ 1978 The development of the reproductive organs of the male giraffe, *Giraffa camelopardalis*. *Journal of Reproduction and Fertility* **52** 1–7. (doi:10.1530/jrf.0.0520001)

Hay MF & Allen WR 1975 An ultrastructural and histochemical study of the interstitial cells in the gonads of the fetal horse. *Journal of Reproduction and Fertility. Supplement* **23** 557–561.

Hradecký P, Benirschke K & Stott GG 1987 Implications of the placental structure compatibility for interspecies embryo transfer. *Theriogenology* **28** 737–746. (doi:10.1016/0093-691X(87)90290-1)

Isobe N, Nakao T, Shimada M, Fukumoto Y, Watanabe H, Minami S, Noda A & Yoshimura Y 2007 Fecal progestagens and estrone during pregnancy in a giraffe: a case report. *Journal of Reproduction and Development* **53** 159–164. (doi:10.1262/jrd.18030)

Kayanja FIB & Blankenship LH 1973 The ovary of the giraffe, *Giraffa camelopardalis*. *Journal of Reproduction and Fertility* **34** 305–313. (doi:10.1530/jrf.0.0340305)

Kellas LM, van Lennep EW & Amoroso EC 1958 Ovaries of some foetal and prepubertal giraffe (*Giraffa camelopardalis* [Linnaeus]). *Nature* **181** 487–488. (doi:10.1038/181487a0)

Lostutoff NM, Walker L, Ott-Joslin JE, Raphael BL & Lasley BL 1986 Urinary steroid evaluations to monitor ovarian function in exotic ungulates. II: comparison between the giraffe (*Giraffa camelopardalis*) and the okapi (*Okapia johnstoni*). *Zoo Biology* **5** 331–338. (doi:10.1002/zoo.1430050403)

Ludwig KS 1962 Beitrag zum Bau des Giraffen Placenta. *Acta Anatomica* **48** 206–223. (doi:10.1159/000141840)

Lueders I, Niemuller C, Pootoolal J, Rich P, Gray C, Streich WJ & Hildebrandt TB 2009*a* Sonomorphology of the reproductive tract in male and pregnant and non-pregnant female Rothschild's giraffes (*Giraffe camelopardalis rothschildi*). *Theriogenology* **72** 22–31. (doi:10.1016/j.theriogenology.2009.01.016)

Lueders I, Hildebrandt TB, Pootoopal J, Rich P, Gray C & Niemuller C 2009*b* Ovarian ultrasonography correlated with fecal progestins and estradiol during the estrous cycle and early pregnancy in giraffes (*Giraffa camelopardalis rothschildi*). *Biology of Reproduction* **81** 989–995. (doi:10.1095/biolreprod.109.077743)

Malassiné A & Leiser R 1984 Morphogenesis and fine structure of the near-term placenta of *Talpa europaea*: I. Endotheliochorial labyrinth. *Placenta* **5** 145–158. (doi:10.1016/S0143-4004(84)80058-2)

Martel C, Melner MH, Gagne D, Simard J & Labrie F 1994 Widespread tissue distribution of steroid sulphatase, 3β-hydroxysteroid dehydrogenase/Δ^5-Δ^4 isomerase (3β-HSD), 17β-HSD 5α-reductase and aromatase activity in the rhesus monkey. *Molecular and Cellular Endocrinology* **104** 103–111. (doi:10.1016/0303-7207(94)90056-6)

Mattner PE & Thorburn GD 1971 Progesterone *in utero*-ovarian venous plasma during pregnancy in ewes. *Journal of Reproduction and Fertility* **24** 140–141. (doi:10.1530/jrf.0.0240140)

McNatty KP, Smith P, Hudson NL, Heath DA, Tisdall DJ, O WS & Braw-Tal R 1995 Development of the sheep ovary during fetal and early neonatal life and the effect of fecundity genes. *Journal of Reproduction and Fertility. Supplement* **49** 123–135.

Meadows S, Allen WR & Antczak DF 1995 Factors affecting the maturation and invasiveness *in vitro* of chorionic girdle cells of different genotypes. *Biology of Reproduction Monograph Series* **1** 171–180.

Mossman HW 1987 Artiodactyl. In *Vertebrate Fetal Membranes*, pp 279–291. Ed HW Mossman. Basingstoke, Hampshire, UK: Macmillan Press Ltd.

Prasad MR, Mossman HW & Scott GL 1979 Morphogenesis of the fetal membranes of an American mole, *Scalopus aquaticus*. *American Journal of Anatomy* **155** 31–68. (doi:10.1002/aja.1001550104)

Rawlings NC, Evans AC, Honaramooz A & Bartlewski PM 2003 Antral follicle growth and endocrine changes in prepubertal cattle, sheep and goats. *Animal Reproduction Science* **78** 259–270. (doi:10.1016/S0378-4320(03)00094-0)

Reimers TJ, Ullmann MB & Hansel W 1985 Progesterone and prostanoid production by bovine binucleate trophoblastic cells. *Biology of Reproduction* **33** 1227–1236. (doi:10.1095/biolreprod33.5.1227)

Rhee HS, Oh SH, Ko BJ, Han DM, Jeon BH, Park H, Moon HB & Kim WS 2003 Expression of 3β-hydroxysteroid dehydrogenase and P450 side chain cleavage enzyme in the human endometrium. *Experimental and Molecular Medicine* **35** 160–166. (doi:10.1038/emm.2003.22)

Schuler G, Wirth C, Klisch K, Pfarrer C, Leiser R & Hoffmann B 1999 Immunolocalization of progesterone receptors in bovine placentomes throughout mid and late gestation and at parturition. *Biology of Reproduction* **61** 797–801. (doi:10.1095/biolreprod61.3.797)

Seki M, Hara Y, Sekiya M, Itagaki T, Hirato K, Yanaihara T & Nakayama T 1987 Changes in the steroid enzyme activity in the human endometrium during the menstrual cycle. *Nippon Sanka Fujinka Gakkai Zasshi* **39** 1571–1578.

Skinner JD & Hall-Martin AJ 1975 A note on foetal growth and development of the giraffe *Giraffa camelopardalis giraffa. Journal of Zoology* **177** 73–79. (doi:10.1111/j.1469-7998.1975.tb05971.x)

Tang B, Markiewicz L, Kloosterboer HJ & Gurpide E 1993 Human endometrial 3β-hydroxysteroid dehydrogenase/isomerase can locally reduce intrinsic estrogenic/progestagenic activity ratios of a steroidal drug (Org OD14). *Journal of Steroid Biochemistry and Molecular Biology* **45** 345–351. (doi:10.1016/0960-0760(93)90003-F)

Ullman MB & Reimers TJ 1989 Progesterone production by binucleate trophoblastic cells of cows. *Journal of Reproduction and Fertility. Supplement* **37** 173–179.

Wango EO, Heap RB & Wooding FB 1991 Progesterone and 5 β-pregnanediol production by isolated fetal placental binucleate cells from sheep and goats. *Journal of Endocrinology* **129** 283–289. (doi:10.1677/joe.0.1290283)

Wilkinson JF & De Fremery P 1940 Gonadotrophic hormones in the urine of the giraffe. *Nature* **146** 491. (doi:10.1038/146491a0)

Wilson VJ 1969 The large mammals of the Matopos National Park. *Arnoldia Rhodesia* **4** 1–32.

Wooding FB 1992 Current topic: the synepitheliochorial placenta of ruminants: binucleate cell fusions and hormone production. *Placenta* **13** 101–113. (doi:10.1016/0143-4004(92)90025-O)

Wooding FB & Burton G 2008 Synepitheliochorial placentation: ruminants (ewe and cow). In *Comparative Placentation*, ch 6, pp 133–167. Eds FB Wooding & G Burton. Heidelburg Berlin: Springer-Verlag. (doi:10.1007/978-3-540-78797-6_6)

Zaho HF, Labrie C, Simard J, Launoit Y, Trudel C, Martel C, Rheaume E, Dupont E, Luu-The V, Pelletier G *et al.* 1991 Characterisation of 3β-hydroxysteroid dehydrogenase/Δ^5-Δ^4 isomerase cDNA and differentiation tissue-specific expression of the corresponding mRNAs in steroidogenic and peripheral tissues. *Journal of Biological Chemistry* **266** 583–593.